Technical University of Denmark

DTU

A stretch-tunable plasmonic structure with a polarization-dependent response

Zhu, Xiaolong; Xiao, Sanshui ; Shi, Lei; Liu, Xiaohan; Zi, Jian; Hansen, Ole; Mortensen, N. Asger

DTU Library
Technical Information Center of Denmark

A stretch-tunable plasmonic structure with a polarization-dependent response

Xiaolong Zhu,[1,2] **Sanshui Xiao,**[1,*] **Lei Shi,**[2] **Xiaohan Liu,**[2] **Jian Zi,**[2] **Ole Hansen,**[3] **and N. Asger Mortensen**[1]

[1]*Department of Photonics Engineering, Technical University of Denmark, DK-2800 Kgs. Lyngby, Denmark*
[2]*Department of Physics, Key Laboratory of Micro and Nano Photonic Structures (Ministry of Education), and State Key Laboratory of Surface Physics, Fudan University, Shanghai 200433, China*
[3]*Department of Micro- and Nanotechnology and Danish National Research Foundation's Center for Individual Nanoparticle Functionality (CINF), Technical University of Denmark, DK-2800 Kgs. Lyngby, Denmark*

[*]*saxi@fotonik.dtu.dk*

Abstract: We experimentally demonstrate a stretchable plasmonic structure composed of a monolayer array of gold semishells with dielectric cores on an elastic PDMS substrate. The composite structure is fabricated using simple and inexpensive self-assembly and transfer-printing techniques, and it supports Bragg-type surface plasmon resonances whose frequencies are sensitive to the arrangement of the metallic semishells. Under uniaxial stretching, the lattice symmetry of this plasmonic structure can be reconfigured from hexagonal to monoclinic, leading to resonance frequency shifts from 200 THz to 191 THz for the TM polarization and from 200 THz to 198 THz for the TE polarization with a strain up to 20%, respectively. Compared with previously reported tunable plasmonic structures, the reconfiguration of lattice symmetry offers a promising approach to tune the surface plasmon resonance with a polarization-dependent response at the standard telecommunication band, and such tunable plasmonic structure might be exploited in realizing photonic devices such as sensors, switches and filters.

© 2012 Optical Society of America

OCIS codes: (240.6680) Surface plasmons; (260.3910) Metal optics; (260.5740) Resonance.

References and links

1. S. A. Maier, *Plasmonics: Fundamentals and Applications* (Springer, 2007).
2. W. L. Barnes, A. Dereux, and T. W. Ebbesen, "Surface plasmon subwavelength optics," Nature **424,** 824–830 (2003).
3. J. Homola, "Surface plasmon resonance sensors for detection of chemical and biological species," Chem. Rev. **108,** 46–493 (2008).
4. S. Xiao, L. Peng, and N. A. Mortensen, "Enhanced transmission of transverse electric waves through periodic arrays of structured subwavelength apertures," Opt. Express **18,** 6040–6047 (2010).
5. M. W. Knight, H. Sobhani, P. Nordlander, and N. J. Halas, "Photodetection with active optical antennas," Science **332,** 702–704 (2011).
6. R. F. Oulton, V. J. Sorger, T. Zentgraf, R. Ma, C. Gladden, L. Dai, G. Bartal, and X. Zhang, "Plasmon lasers at deep subwavelength scale," Nature **461,** 629–632 (2009).
7. H. A. Atwater and A. B. Polman, "Plasmonics for improved photovoltaic devices," Nat. Mat. **9,** 205–213 (2006).
8. X. Zhang, B. Sun, J. M. Hodgkiss, and R. H. Friend, "Tunable ultrafast optical switching via waveguided gold nanowires," Adv. Mater. **20,** 4455–4459 (2008).

9. C. Jeppesen, S. S. Xiao, N. A. Mortensenb, and A. Kristensen, "Extended verification of scaling behavior in split-ring resonators," Opt. Commun. **284,** 799–801 (2011).
10. W. Dickson, G. A. Wurtz, P. R. Evans, R. J. Pollard, and A. V. Zayats, "Electronically controlled surface plasmon dispersion and optical transmission through metallic hole arrays using liquid crystal," Nano Lett. **8,** 281–286 (2008).
11. H. L. Chen, K. C. Hsieh, C. H. Lin, and S. H. Chen, "Using direct nanoimprinting of ferroelectric films to prepare devices exhibiting bi-directio nally tunable surface plasmon resonances," Nanotechnology **19,** 435304 (2008).
12. G. Xu, C. M. Huang, M. Tazawa, P. Jin, and D. M. Chen, "Nano-Ag on vanadium dioxide. II. Thermal tuning of surface plasmon resonance," J. Appl. Phys. **104,** 053102 (2008).
13. Y. L. Chiang, C. W. Chen, C. H. Wang, C. Y. Hsieh, Y. T. Chen, H. Y. Shih, and Y. F. Chen, "Mechanically tunable surface plasmon resonance based on gold nanoparticles and elastic membrane polydimethylsiloxane composite," Appl. Phys. Lett. **96,** 041904 (2010).
14. S. Olcum, A. Kocabas, G. Ertas, A. Atalar, and A. Aydinli, "Tunable surface plasmon resonance on an elastomeric substrate," Opt. Express **17,** 8542–8547 (2009).
15. R. M. Cole, S. Mahajan, and J. J. Baumberg, "Stretchable metal-elastomer nanovoids for tunable plasmons," Appl. Phys. Lett. **95,** 154103 (2009).
16. X. L. Zhu, L. Shi, X. H. Liu, J. Zi, and Z. L. Wang, "A mechanically tunable plasmonic structure composed of a monolayer array of metal-capped colloidal spheres on an elastomeric substrate," Nano Res. **3,** 807–812 (2010).
17. J. Sun, C. J. Tang, P. Zhan, Z. L. Han, Z. S. Cao, and Z. L. Wang, "Fabrication of centimeter-sized single-Domain two-dimensional colloidal crystals in a wedge-shaped cell under capillary forces," Langmuir **26,** 7859–7864 (2010).
18. Y. Ding, S. Garland, M. Howland, A. Revzin, and T. Pan, "Universal nanopatternable interfacial bonding," Adv. Mater. **23,** 5551–5556 (2011).
19. S. Xiao, J. J. Zhang, L. Peng, C. Jeppesen, R. Malureanu, A. Kristensen, and N. A. Mortensen, "Nearly zero transmission through periodically modulated ultrathin metal films," Appl. Phys. Lett. **97,** 071116 (2010).
20. T. A. Kelf, Y. Sugawara, R. M. Cole, and J. J. Baumberg, "Localized and delocalized plasmons in metallic nanovoids," Phys. Rev. B **74,** 245415 (2006).
21. Q. G. Wang, C. J. Tang, J. Chen, P. Zhan, and Z. L. Wang, "Effect of symmetry breaking on localized and delocalized surface plasmons in monolayer hexagonal-close-packed metallic truncated nanoshells," Opt. Express **19,** 23889–23900 (2011).
22. N. S. King, Y. Li, C. Ayala-Orozco, T. Brannan, P. Nordlander, and N. J. Halas, "Angle- and spectral-dependent light scattering from plasmonic nanocups," ACS Nano **5,** 7254–7262 (2011).
23. P. V. Dorpe and J. Ye, "Semishells: versatile plasmonic nanoparticles," ACS Nano **5,** 6774–6778 (2011).
24. L. Shi, H. W. Yin, X. L. Zhu, X. H. Liu, and J. Zi, "Direct observation of iso-frequency contour of surface modes in defective photonic crystals in real space," Appl. Phys. Lett. **97,** 251111 (2010).
25. CST Microwave Studio, CST GmbH, Germany.

1. Introduction

Due to the oscillations of free electrons at metal interfaces, plasmonic nanostructures can concentrate optical fields into nanoscale volumes [1, 2]. The concentration of optical fields and sub-wavelength nature can render important applications from biological and chemical sensors [3] to devices for sub-wavelength manipulation of light [4], photo detection [5], lasers [6] and solar energy harvesting [7]. The optical response of a conventional plasmonic structure is usually determined by the shape and size of the metal structure, the type of metal or the refractive index of the surrounding materials, and it is generally unchanged once fabricated. The response of essentially passive plasmonics can be rendered actively by integrating dynamic components into the structure. To date, tuning the optical response of plasmonic structures has been limited in special ranges due to optical [8], fluidic [9], electronic [10], ferroelectric [11] and thermal [12] tuning mechanisms involved. Stretchable plasmonic structures have generated increasing interest for actively tuning optical response in a reproducible and continuous way. Through mechanical deformation of elastomeric substrates, spectral shifts in the resonance of plasmonic structures are reported, such as in nanoparticles matrix [13], gratings [14] and metal nanovoids [15]. However, most of the stretch-tunable plasmonics rely on modifying the gaps or cavities within or between the resonant elements which leads to limited working wavelengths.

In this paper, we illustrate a simple and inexpensive method based on self-assembly and lift-transfer techniques [16] to fabricate a new type of large-area, narrow-band and stretch-tunable
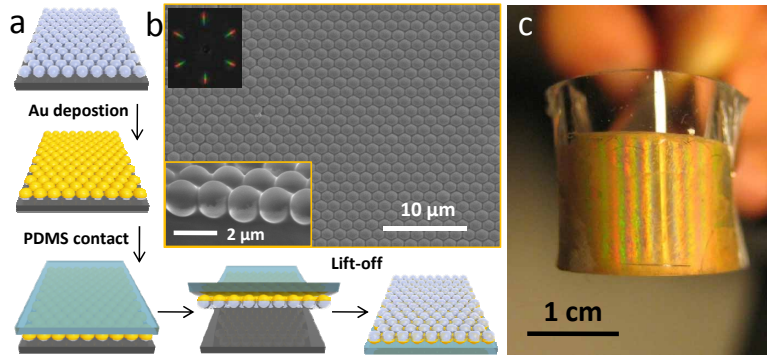
Fig. 1. (a) Scheme for fabricating two-dimensional arrays of opening-up gold semishells with PS cores. (b) Top-down and cross-sectional (lower inset) scanning electron microscopy (SEM) images of a gold semishell array on a PDMS substrate and a light diffraction pattern (left-upper inset). The diameter of the PS core is 1.5 μm. (c) Optical micrograph of a fabricated sample with wafer-scale area and high flexibility.

plasmonic semishells, composed of a dielectric core and a thin metallic shell and arranged in a monolayer hexagonal-close-packed array on an elastomeric substrate. This composite structure supports delocalized surface plasmon (SP) modes. By breaking the lattice symmetry other than enlarging the sizes of gaps or cavities under strain, we can realize not only a large frequency shift but also a polarization dependence at telecommunication wavelengths.

2. Fabrication

Figure 1(a) depicts the fabrication scheme used to generate a narrow-band stretchable plasmonic structure with wafer-scale area. In the first step, a monolayer hexagonal-close-packed array of monodisperse polystyrene (PS) spheres with a diameter of 1500 nm (size dispersion 2%) was formed on a pre-treated silicon surface by a self-assembly method [17]. After that, a 35-nm-thick gold film was deposited on the monolayer array of PS spheres by E-beam evaporation. Due to the shadow effect, metallic caps can be formed on the PS spheres to produce the semishells with PS cores.

The second step was to prepare an elastomeric substrate. A 2-mm-thick transparent polydimethylsiloxane (PDMS) (Sylgard 184, Dow Corning; the mixing ratio between the polymer precursor and the curing agent was 10:1.0) layer was spread on another quartz slide and left to cure at 65 °C for 4 hours. After curing, the PDMS membrane was carefully peeled off the slide. The third step was to transfer the monolayer array of gold capped PS spheres onto the PDMS substrate. To do this, the PDMS film was pasted onto the monolayer semishells array prepared in the first step. The PDMS film was then carefully lifted off, such that the monolayer array of gold capped PS spheres can be transferred completely onto the PDMS substrate. This is possible, because of the stronger static force between the gold caps and the neat PDMS surface (like adhesive tape) compared to the interaction between the colloidal spheres and the Si surface [18]. Therefore, we can successfully accomplish the preparation of the gold semishells array with the opening facing up on a PDMS substrate, as shown in Fig. 1(b).

3. Results and discussions

Figure 1(b) illustrates top-down and cross-sectional images of a portion of opening up gold semishell arrays on a PDMS substrate. We can find that these gold semishells with PS cores are arranged regularly in a hexagonal lattice confirmed by the six-fold light diffraction pattern, as
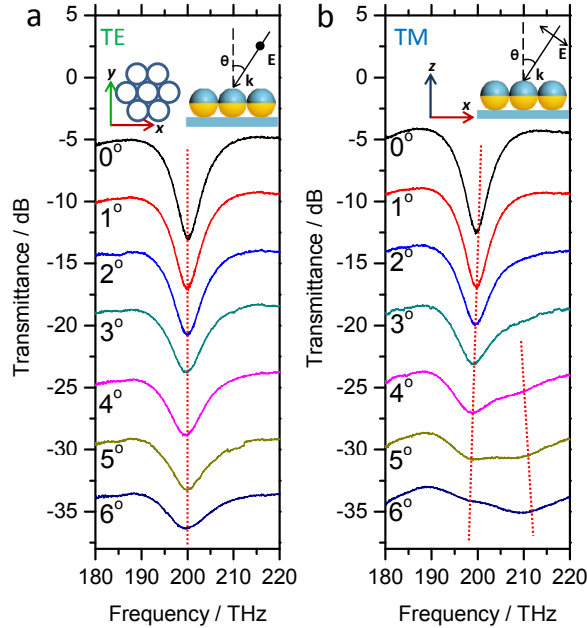
Fig. 2. Transmittance spectra of the plasmonic structure at different incident angles measured by free-space optical spectroscopy for the (a) TE and (b) TM polarization. For clarity, the individual spectra have been displaced by -5 dB. Dotted lines indicate transmission dip shifts corresponding to the angle-dependent resonance of coupled surface plasmons. Insets are sketches of the arrayed gold semishells with PS cores on a PDMS substrate with coordinates.

shown in the left-upper inset in Fig. 1(b). Figure 1(c) highlights typical sample size and high flexibility. Strong diffraction can be observed from the two-dimensional (2D) hexagonal lattice of gold semishells array on the optically transparent PDMS film.

The transmittance, shown in Fig. 2, for the fabricated device, was measured by a free-space setup using a supercontinuum light source (500-1750 nm, SuperK SCB-Compact 100-PC) and a spectrum analyzer (400-1750 nm, Ando AQ-6315E). Details of the setup can be found in Ref. [19]. The narrow-band resonances around 200 THz (1.5 μm) under the normal incidence for both polarizations are caused by a delocalized Bragg-type SP mode that relies on a strong near-field interaction between adjacent gold semishells. When these semishells are put together to form a regular 2D lattice, SP resonances between neighboring semishells can couple with each other provided that the spatial distance is not large enough. Due to the periodicity of the 2D lattice, this coupling leads to a well defined dispersion of SPs or band structure $\omega(K_{sp})$, where K_{sp} is the wave-vector of the coupled SPs. If the in-plane component of incident light wave vector $K_{\parallel}$ satisfies the following phase-matching condition [1, 2]:

$$K_{sp} = K_{\parallel} + G_{mn} \qquad (1)$$

then coupled SPs can be excited, where $G_{mn} = 2\pi/\Lambda$ represents the reciprocal lattice vectors of the 2D lattice. By using the weak scattering approximation [20, 21], the close-packed nature of the surface leads to diffraction from the planes of scatters, which are spaced by a distance $\Lambda = \sqrt{3}/2(m\mathbf{a} + n\mathbf{b})$, where m and n are integers and $\mathbf{a}$ and $\mathbf{b}$ are two basis lattice vectors in this 2D hexagonal array.

The above model has been verified by experimental data of far-field angle-resolved trans-

mittance spectra. As seen in Fig. 2(a), for the transverse-electric (TE, electric field polarized along the y-direction) polarized light, the excited in-plane plasmon mode does not depend on the incident angle. This is because the in-plane component of the electric field of the incident light remains unchanged with various incident angles. But for the transverse-magnetic (TM, the electric field polarized along the x-direction) polarized light, one can see that the single transmission resonance around 200 THz under the normal incidence splits into two branches at small-angle oblique incidence whose positions are all angle-dependent, indicating the delocalized nature of this mode (Fig. 2(b)). Moreover, the outstanding angular sensitivity attributed to the symmetry-broken metallic semishells can open up applications such as infrared angular sensors or modulators [22, 23].

To demonstrate tunability of our stretchable plasmonic structure, uniaxial strain is applied along the x-direction on a stress stage which is in the optical path of the free-space measurement setup. Transmittance spectra can be recorded and the six-fold light diffraction pattern is used to confirm the orientations related to the ordered lattice synchronously.
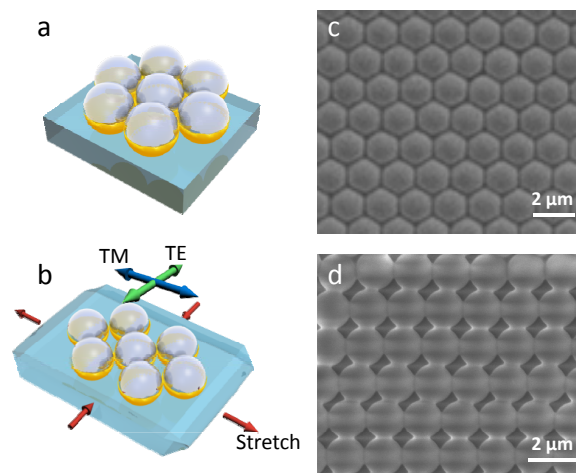

Fig. 3. Schematic illustrations and their corresponding SEM images of the plasmonic structures (a, c) before and (b, d) after uniaxial strain applied along the x-direction.

Figures 3(a) and 3(b) show the schematic illustrations of the structure before and after the strain is applied, respectively. Corresponding SEM images are also captured as shown in Figs. 3(c) and 3(d). Uniaxial strain along the x-direction changes the six-fold lattice symmetry because of the anisotropic responses of the PDMS substrate. The lattice constant along the x-direction enlarges significantly while the one along the y-direction compresses a little (Figs. 3(b) and 3(d)).

Because of the tight coupling between lattice structures and optical properties for delocalized Bragg-type SPs, the stretch induced anisotropic behavior extends to the optical domain. We traced the transmittance spectra as a function of strain for both TE and TM polarized light, see Fig. 4(a). As the transmission dips are caused by the coupled SPs between neighboring gold semishells which are highly dependent on the lattice constant along the electric field. A larger lattice constant results in a lower resonance frequency by relating the real-space and reciprocal-space lattices. As shown in Fig. 3(d), the lattice is no longer hexagonal and deformed into a lower-symmetry monoclinic lattice when strained. This results in a red shift of the transmission dip (from 200 THz to 191 THz with a strain up to 20%) for the TM polarized light incidence as the effective coupling distance between two adjacent semishells increases along the stretching direction. For the TE polarized light which is perpendicular to the stretching direction, the
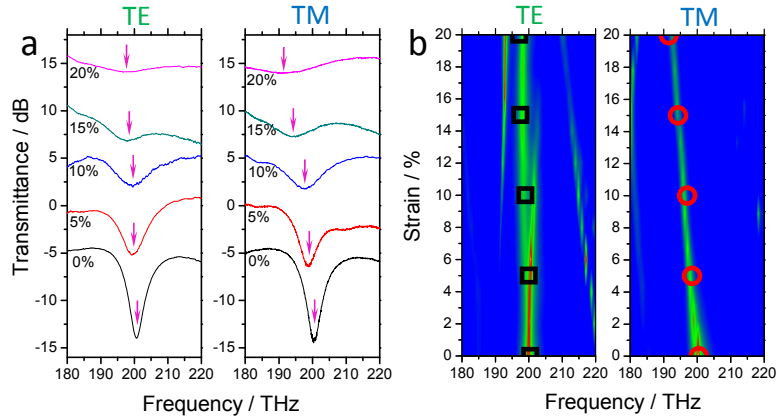
Fig. 4. (a) Transmittance spectra of the stretchable plasmonic structure under different applied strain for both TE and TM polarized light. The individual spectra have been displaced by +5 dB for clarity. Arrows indicate transmission dip shifts corresponding to stretch-tunable plasmonic resonances. (b) Simulated transmittance spectra maps as a function of strain where the squares and circles represent the measured transmission dips for both TE and TM polarization, respectively.

transmission dip shifts much less (from 200 THz to 198 THz with a strain up to 20%) as the effective coupling distance changes only slightly. It is worthy to mention that, because of the inevitable defects in self-assembled structures [24], a mechanical strain will cause a nonuniform lattice of the plasmonic structure. Therefore, the plasmonic resonance will smear out in the measured results as deformation increases (see Fig. 4(a)). The strain-induced polarization-dependent effects of the tunable plasmonic structure are also verified by numerical simulations (performed with the aid of a commercially available finite integration method [25]), as shown in Fig. 4(b), where the squares and circles represent the measured resonance dip positions for the TE and TM polarization, respectively. The positions of the measured resonance dips illustrate a good agreement with those obtained by the numerical simulations.

4. Conclusion

We have demonstrated a stretchable plasmonic structure consisting of a monolayer array of gold semishells with PS cores on an elastic PDMS substrate using self-assembly and lift-transfer techniques. The delocalized Bragg-type SP resonances with outstanding angular sensitivity may be used as infrared angular sensors or modulators. Besides, it can be mechanically tuned by breaking the lattice symmetry under strain. Experimental results show that the transmission dip, associated with the Bragg-type SP resonance, shifts from 200 THz to 191 THz for the TM polarization and from 200 THz to 198 THz for the TE polarization when a strain up to 20% is applied respectively, indicating polarization dependent tunability of our plasmonic structure. Measured results have been confirmed by the numerical simulations. The stretch-tunable plasmonic structure with a polarization dependent response at 1.5 μm region can be potentially used in sensing, switching, and filtering for telecommunication.

Acknowledgments